Wehrli, B. (1990): Redox Reactions of Metal Ions at Mineral Surfaces. – In: Stumm, W. (ed) Aquatic Chemical Kinetics – Reaction Rates of Processes in Natural Waters. – p. 311-336, 9 Abb., 4 Tab.

11

REDOX REACTIONS OF METAL IONS AT MINERAL SURFACES

Bernhard Wehrli

Lake Research Laboratory, Institute for Water Resources and Water Pollution Control (EAWAG), Kastanienbaum, Switzerland; Swiss Federal Institute of Technology (ETH), Zürich, Switzerland

1. INTRODUCTION

1.1. Reactions at Geochemical Redox Boundaries

The presence of dissolved molecular oxygen in natural waters establishes a low level of chemically reactive electrons. As a consequence, dissolved and adsorbed metal ions are found in their higher oxidation states in oxic waters. The geochemical cycling of electrons on a global scale is dominated by photosynthesis and respiration with an electron flux in the order of 42 moles of electrons per square meter per year at the sea surface (Stumm, 1978). The reduced products of such photosynthetic activity accumulate at the bottom of rivers and lakes. Fast degradation of organic material and slow supply of dissolved oxygen produce steep redox gradients at the sediment–water interface. Similar oxic–anoxic transition zones are found at the boundaries of polluted groundwater plumes and at reduced mineral layers in soils.

Unknown redox kinetics often limit the predictive value of calculated redox equilibria in the aquatic environment. Thermodynamics indicate that manganese should be present in oxic waters as Mn(IV) oxide. However, in a long-term experiment Diem and Stumm (1984) have shown that Mn^{2+} is not oxidized by O_2 within several years (Fig. 1*a*). Microorganisms usually catalyze such slow redox reactions if the concentrations involved are high enough. Recently experimental evidence has been accumulated that aqueous mineral surfaces provide additional accelerated pathways for redox processes such as the oxygenation of metal ions (Davies and Morgan, 1989; Wehrli and Stumm, 1988) and the oxidation of organic pollutants (Stone, 1986). The manganese oxygenation is accelerated by iron oxide particles by a factor of more than 10^4

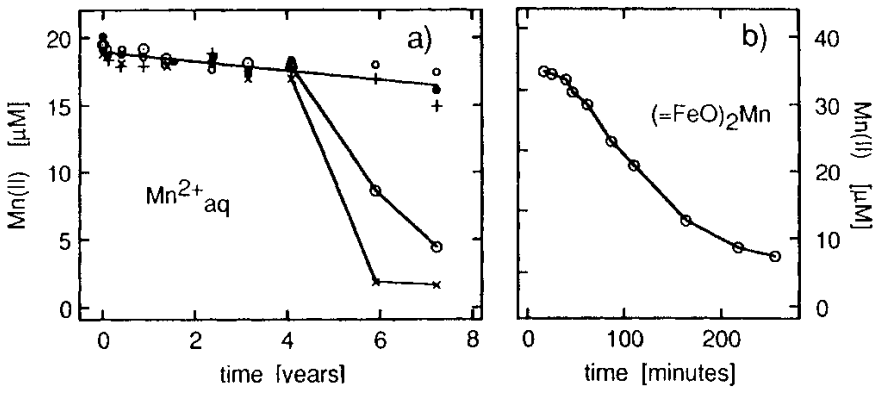

Figure 1. Oxygenation of Mn(II): (*a*) homogeneous solution at pH 8.4, data from Diem and Stumm (1984); (*b*) 10 m*M* goethite suspension at pH 8.5, data from Davies and Morgan (1989). The surface complex reacts within hours, whereas the homogeneous Mn(II) solutions are stable for years.

(Fig. 1*b*). Iron and manganese particles often accumulate at redox boundaries (Davison, 1985; De Vitre et al., 1988) and supply reactive mineral surfaces in zones with high chemical electron fluxes. Oxidation–reduction reactions of metal ions at mineral surfaces thus play a key role in the "geochemical cycling of electrons". The distribution and fate of many inorganic species is coupled with the reductive dissolution and the oxidative precipitation of manganese and iron at redox boundaries.

Applications of redox reactions on mineral surfaces in areas such as water treatment have been reviewed by Segal and Sellers (1984); Voudrias and Reinhard (1986) discussed the organic transformations at the solid–liquid interface. Here the discussion is confined to selected inorganic redox reactions. Table 1 lists some of the more important heterogeneous processes of inorganic

TABLE 1. Examples of Inorganic Redox Reactions on Mineral Surfaces[a]

Process	Oxidant	Reductant	Reference[b]
Heterogeneous equilibrium	FeOOH, MnOOH	Fe^{2+}, Mn^{2+}	
Oxidative adsorption	MnO_x	Fe(II), Co(II), Sn(II)	1
Reductive dissolution	MnO_x, FeOOH	U(IV), Cr(III), organics	2
Oxidation of pyrite	O_2, Fe(III)	FeS_2	3
Heterogeneous oxygenation	O_2	Adsorbed Fe(II), Mn(II), V(IV)	4

[a] Manganese and iron oxides act as electron acceptors; sulfides and reduced metal ions adsorbed to particles are heterogeneous reductants.

[b] References: (1) see Dillard and Schenk (1986) and references, cited therein. (2) Gordon and Taube (1962), Van der Weijden and Reith (1982), Stone (1986), Sulzberger (Chapter 14, this volume), (3) Lowson (1982), Luther (Chapter 6, this volume), (4) Tamura et al. (1976), Davies and Morgan (1989), Wehrli and Stumm (1988).

species in natural waters. Solid-dissolved equilibria such as

$$Fe^{III}OOH_{(s)} + 3H^+ + e^- \Leftrightarrow Fe^{2+} + 3H_2O \quad (1a)$$

are easily calculated from thermodynamic data. However, a mechanistic discussion of heterogeneous reaction rates should be based on the redox potential of elementary reaction steps such as the reduction of a surface Fe(III) center:

$$=Fe^{III}OH_2^+ + e^- \Leftrightarrow =Fe^{II}OH_2 \quad (1b)$$

In this chapter I will propose a kinetic estimate for the thermodynamics of reactions like Eq (1b). The solid phases listed in Table 1 may act as a reductant or an oxidant. One of the prominent geochemical electron donors is pyrite. From an estimate of global pyrite weathering of 36 Tg y^{-1} (Garrels et al., 1973) we may deduce an average electron flux on the land surface in the order of 0.02 mol m^{-2} y^{-1}. At redox boundaries in salt marshes and in lake sediments microbial sulfate reduction will intensify this "electron cycling." Luther (Chapter 6, this volume) discusses the details of sulfide redox mechanisms.

In contrast to pyrite, the hydroxides of iron and manganese act as electron acceptors. An adsorbed reducing agent may follow two different pathways after electron transfer to these mineral surfaces. Oxidation products with high particle affinity such as Fe(III) (Koch, 1957), Cr(III) (Zabin and Taube, 1964), Co(III) (Crowther et al., 1983), Sn(IV) (Rapsomanikis and Weber, 1985) will form strong surface complexes. Such an oxidative adsorption consumes the available mineral surface. If the oxidation products are anions such as Cr(VI) (Van der Weijden and Reith, 1982), As(V) (Oscarson et al., 1981) or organic compounds, which desorb more easily, the reactive interface is regenerated continuously and the reductive dissolution of the solid phase dominates the process. Stone (1986) studied the dissolution of manganese oxides in presence of reducing organic compounds. An account on the influence of light on this process is given by Sulzberger (Chapter 14, this volume). A last group of heterogeneous redox reactions involves species adsorbed to "innocent" surfaces such as Al_2O_3 or SiO_2 and silicates. Davies and Morgan (1989) observed acceleration of the Mn(II) oxygenation (Fig. 1*b*) also in the presence of silica and alumina, which have no accessible lower oxidation states. They attributed the accelerating kinetic effect to the change in coordination, when Mn^{2+} becomes adsorbed.

1.2. Two Paradigms

Mineral surfaces are rather complex reaction media. Two complementary paradigms have served so far as starting points for mechanistic discussions of reactions at the mineral–water interface: The concept of the solid–aqueous interface as an electrode and the picture of the mineral surface as a two-dimensional array of surface complexes. Both points of view are exploited in this chapter.

Marcus' theory (1965) has long been used to compare outer-sphere redox reactions in homogeneous solution with corresponding electrode kinetics. Recent theoretical developments by Astumian and Schelly (1984) allow the general comparison of homogeneous and heterogeneous rate constants. Such simple kinetic models account only for the change in geometry that accompanies the adsorption from solution to a two-dimensional surface and the electrostatic contribution from the diffuse double layer surrounding the mineral grains.

A discussion of specific catalytic effects of mineral surfaces must be based on thermodynamic and structural information of the reactive surface species. The first part includes a brief outline of the emerging picture of mineral surfaces as two-dimensional arrays of surface complexes. This part assembles also the kinetic tools that are useful for comparison of the reactivity of aqueous metal ions and their adsorbed surface complexes. The second part presents a reevaluation of the most extensively studied inorganic redox reactions in natural waters: the oxygenation of VO^{2+}, Mn^{2+}, Fe^{2+} and Cu^{+} in homogeneous and heterogeneous systems.

2. HETEROGENEOUS ELECTRON TRANSFER

A vast literature exists on the kinetics and mechanisms of electron-transfer reactions between dissolved metal ions. A recent review was written by Sutin (1986). Physical chemists, however, have dealt so far almost exclusively with reactions in aqueous solution of very low pH or high ligand concentrations. Such studies have shown that the *homogeneous* electron-transfer between couples such as Fe(III)/Fe(II) proceeds via three distinct steps. First the two reactants diffuse together and form a reactive intermediate called the *precursor complex*. The electron transfer occurs after an appropriate reorganization of the nuclear configuration. This yields a short-lived product called the *successor complex*. Finally the successor decomposes to the separated products of the redox reaction:

$$FeOH^{2+}_{aq} + Fe^{2+}_{aq} \xrightarrow{\text{precursor formation}} [Fe^{III}\text{–}OH\text{–}Fe^{II}]^{4+} \quad (2)$$

$$[Fe^{III}\text{–}OH\text{–}Fe^{II}]^{4+} \xrightarrow{\text{electron transfer}} [Fe^{II}\text{–}OH\text{–}Fe^{III}]^{4+} \quad (3)$$

$$[Fe^{II}\text{–}OH\text{–}Fe^{III}]^{4+} \xrightarrow{\text{dissociation of successor}} Fe^{2+}_{aq} + FeOH^{2+}_{aq} \quad (4)$$

The rate constant of the overall reaction at 25°C is $k = 3.1 \times 10^3\ M^{-1}\,s^{-1}$ (Silverman and Dodson, 1952). In very acidic solution a pH-independent reaction with Fe^{3+} as a reactant is observed. This self-exchange between the aquo complexes proceeds much slower with a rate constant of $4\ M^{-1}\,s^{-1}$. In this case the precursor complex consists probably of a simple encounter complex

without a bridging ligand between Fe^{2+} and Fe^{3+}. The almost thousandfold acceleration of the electron transfer when $FeOH^{2+}$ replaces Fe^{3+} is typical for reactions with OH^- as an electron bridge in the precursor complex (Haim, 1983).

The ferric ion occurs only in trace concentrations in the neutral pH range of natural waters. Therefore, we should realize that the relevant Fe(III)/Fe(II) equilibrium in most aquatic environments involves *heterogeneous* electron transfer between dissolved Fe(II) and the surface centers of iron oxihydroxide particles. A similar three-step mechanism can be written for this process:

$$=Fe^{III}OH + Fe^{2+} \xrightarrow{\text{adsorption}} (=Fe^{III}\text{-}O\text{-}Fe^{II})^+ + H^+ \tag{5}$$

$$(=Fe^{III}\text{-}O\text{-}Fe^{II})^+ \xrightarrow{\text{electron transfer}} (=Fe^{II}\text{-}O\text{-}Fe^{III})^+ \tag{6}$$

$$(=Fe^{II}\text{-}O\text{-}Fe^{III})^+ + H_3O^+ \xrightarrow{\text{desorption}} =Fe^{II}OH_2 + Fe^{III}OH^{2+} \tag{7}$$

An extensive numerical study on such heterogeneous three-step processes has been given by Stone and Morgan (1987). The adsorption–desorption kinetics of divalent metal ions is fast: Yasunaga and Ikeda (1986) report relaxation times in the order of milliseconds to seconds. The pH as a master variable governs the adsorption of Fe(II) in the preceding example. The elucidation of adsorption equilibria and the structure of precursor complexes such as $(=Fe^{III}\text{-}O\text{-}Fe^{II})^+$ at the mineral surface is therefore a prerequisite for the study of heterogeneous redox kinetics.

2.1. Adsorption

Alkali ions and inorganic anions such as NO_3^-, ClO_4^- adsorb electrostatically to mineral surfaces of opposite charge. Such surface species are analogs to outer-sphere complexes (ion pairs) in solution. Transition-metal ions, however, adsorb even against the electrostatic repulsion of a positively charged mineral surface. Figure 2 depicts the adsorption equilibria of vanadyl(IV) and ferrous iron to TiO_2. Both cations adsorb to the positively charged surface (the zero point of charge of anatase is $pH_{ZPC} \sim 6.4$). To explain such observations, Schindler and Stumm (1987) have developed a surface complexation model. The adsorption process is treated as a complex formation reaction, where surface =M–OH– groups replace coordinated water molecules at the adsorbed metal center. The adsorption of a ferrous iron to an anatase surface may be given by equilibria such as

$$2 \equiv Ti\text{-}OH + Fe^{2+} \overset{K_2}{\Leftrightarrow} (\equiv Ti\text{-}O)_2Fe + 2H^+ \tag{8}$$

From correlations between hydrolysis constant and surface complex formation

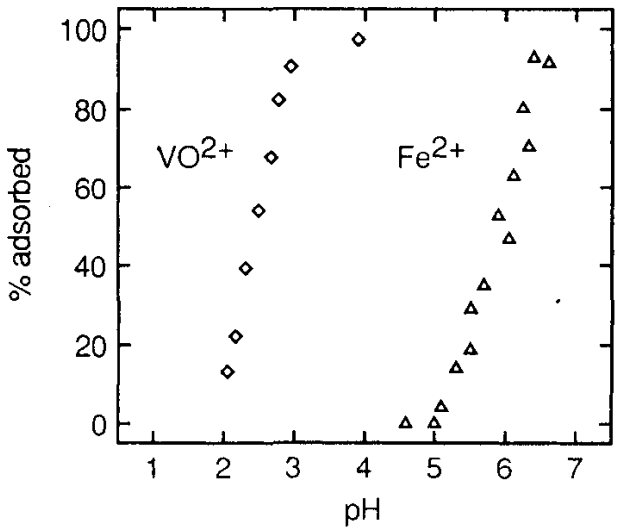

Figure 2. Adsorption of vanadyl and Fe(II) to TiO_2 (anatase). Both cations adsorb specifically to the positively charged surface. Conditions: 25°C, $I = 0.1$ ($NaClO_4$); $[VO^{2+}] = 50\ \mu M$, $2\ g\ L^{-1}$ TiO_2; $[Fe^{2+}] = 100\ \mu M$, $10\ g\ L^{-1}$ TiO_2.

constants (Schindler and Stumm, 1987) we expect that vanadyl ($pK_1^* \sim 6$) adsorbs stronger to an oxide surface than ferrous iron ($pK_1^* \sim 9.5$). Such equilibrium measurements quantify the concentration of reactive surface species. The structural interpretation, however, has to be based on spectroscopic evidence.

Recent ENDOR studies on the adsorption of Cu^{2+} (Rudin and Motschi, 1984) and VO^{2+} (Motschi and Rudin, 1984) have verified the conceptual model of inner-sphere coordination by surface ligands =M–OH. These authors found that the surface groups enter the coordination sphere of the adsorbed metal centers and replace one, two, or more water molecules. Molecular modeling techniques help visualize the possible structural arrangements on mineral surfaces. Figure 3 presents the two-dimensional array of surface ligands on the anatase surface. The available =TiOH groups are lined up in zigzag chains. The local geometry allows the formation of mono-, bi- and even tridentate surface complexes. The coordination of these surface ligands changes the reactivity of surface metal centers in different ways. These ligands act as σ donors and increase the electron density at the metal center, thus stabilizing higher oxidation states. This thermodynamic effect results in a lower redox potential. Such a change in E° may directly affect electron-transfer rates (see below). The well-documented role of oxygen as an electron bridge suggests specific mechanistic effects: bridging surface =M–O groups may mediate electron transfer in a similar way as coordinated OH^- in homogeneous solution (compare Eqs. 3 and 6).

2.2 Two Electron-Transfer Mechanisms

Electron transfer between metal ions may occur either as inner-sphere (is) or an outer-sphere (os) reaction. The first case involves a ligand exchange and the

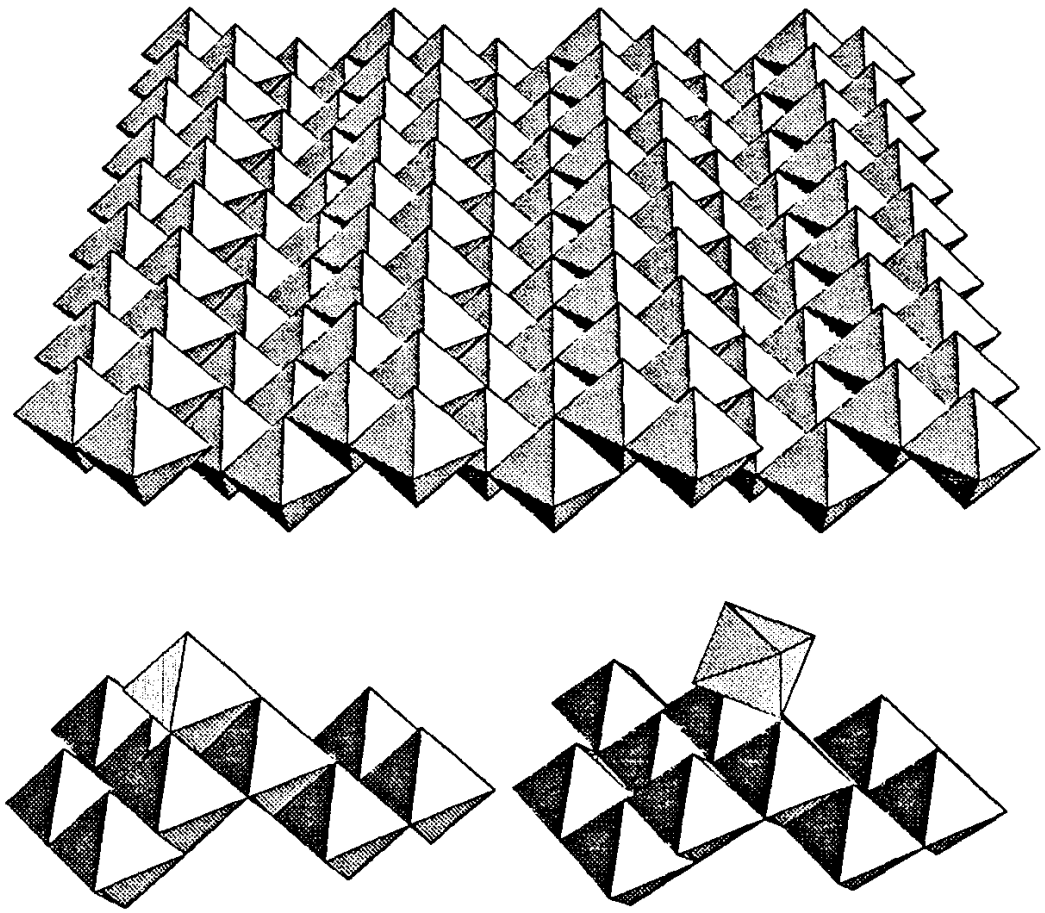

Figure 3. The anatase surface shows zigzag chains of Ti surface octahedra. Each Ti site carries a ≡TiOH ligand that may bind adsorbed metal centers. The two surface groups to the right represent a bidentate (above) and a tridentate surface complex (below).

TABLE 2. Proposed Mechanisms of Reductive Dissolution

Solid	Reductant	Mechanism[a]	Evidence	Reference
α-Fe_2O_3	$V^{II}(pic)_3^-$	os	Diffusion-controlled	Segal and Sellers (1984)
MnO_2	Cr^{II}_{aq}	is	^{18}O tracer	Zabin and Taube (1964)
PbO_2	U^{IV}_{aq}	is	^{18}O tracer	Gordon and Taube (1962)
MnO_2	Fe^{II}_{aq}	is	Saturation effects	Koch (1957)

[a] os = outer-sphere; is = inner-sphere.

coordination of a bridging ligand such as in Eq. 2. An outer-sphere reaction occurs without ligand substitution. Reductive dissolution of oxides with different metal complexes as reductants illustrates the two mechanisms for heterogeneous systems (Table 2). The os mechanism has been assigned to many V^{2+} electron-transfer reactions that proceed faster than the ligand exchange at the V^{2+} center. The "bulky" negatively charged V(II) complex adsorbs electrostatically to the positive hematite surface. The outer-sphere oxidation of the V(II) center (Segal and Sellers, 1984) may be written in analogy to homogeneous systems as

$$=Fe^{III}OH_2^+ + (V^{II}L_3)^- \longrightarrow =Fe^{III}OH_2^+(V^{II}L_3)^-$$

adsorption: ion pair formation

$$=Fe^{III}OH_2^+(V^{II}L_3)^- \longrightarrow =FE^{II}OH_2(V^{III}L_3) \qquad (9)$$

outer-sphere electron transfer

The ^{18}O-tracer studies of Gordon and Taube (1962) on the oxidation of U(IV) on PbO_2 have shown that both oxygen ions in the product UO_2^{2+} are derived from the oxide lattice. This result indicates an inner-sphere mechanism and is compatible with a binuclear U(IV) surface complex:

$$2{=}Pb^{IV}OH + U^{IV} \longrightarrow \begin{matrix} {=}Pb^{IV}O \\ {=}Pb^{IV}O \end{matrix}\!\!>U^{IV} + 2H_3O^+$$

surface complexation

$$\begin{matrix} {=}Pb^{IV}O \\ {=}Pb^{IV}O \end{matrix}\!\!>U^{IV} \longrightarrow \begin{matrix} {=}Pb^{II}O \\ {=}Pb^{IV}O \end{matrix}\!\!>U^{VI} \qquad (10)$$

inner-sphere electron transfer

In the last step the U(VI) desorbs from the surface as a uranyl ion, UO_2^{2+}. Two oxygen ions from the PbO_2 surface remain coordinated to the high valent uranyl. Recently Combes (1989) has shown by EXAFS (extended x-ray absorption fine-structure spectroscopy) that uranyl indeed forms bidentate surface complexes on goethite. The local coordination sites on α-FeOOH are structurally very similar as the PbO_2 sites with a rutile structure.

2.3. The Marcus Relations

Outer-sphere electron transfer is one of the simplest reaction types because no bonds are broken or formed. It is therefore not surprising that this class of reactions was the subject of early kinetic theories. More than 30 years ago Marcus (1965) derived a predictive theory for the rate constants of os redox reactions in homogeneous and heterogeneous systems. A didactic introduction was later given by the same author (Marcus, 1975), and Sutin (1986) reviewed modern refinements of the theory.

The second-order rate constant for electron transfer in solution can be given in terms of the Arrhenius equation

$$k = A \exp(-E_a/RT) \tag{11a}$$

where A stands for the preexponential factor ($M^{-1}\,s^{-1}$) and E_a refers to the activation energy (kJ mol^{-1}). Marcus replaced the factor A by the collision frequency $Z = \kappa k_B T/h$, where κ refers to the transmission coefficient, k_B is Boltzmann's constant, and h is Planck's constant. If every collision leads to a reaction ($\kappa = 1$) and $T = 298$ K, then the collision frequency in homogeneous solution is $Z = 10^{11}\,M^{-1}\,s^{-1}$. In Marcus' theory the activation energy is split into two parts:

1. The two reactants must diffuse together. The work w (kJ mol^{-1}) required for this process is determined by the electrostatic forces between the two reactants. If one reactant (such as O_2) is uncharged the work term can be neglected.
2. Bond distances and bond angles between ions and solvent molecules change on electron transfer. The iron–oxygen bond distances for the aquo complex of Fe^{3+} are 0.13 Å shorter than in the case of Fe^{2+}. Prior to os electron transfer coordinated water molecules in such redox couples are rearranged at an intermediate position. The corresponding reorganization energy ΔG^* contributes as the second term to the activation energy:

$$k = Z \exp[-(w + \Delta G^*)/RT] \tag{11b}$$

Because Z can be calculated from collision theory and w is determined by simple electrostatics, Eq. 11b would allow a prediction of rate constants if a theoretical derivation can be found for the reorganization energy ΔG^*. Based on free-energy surfaces Marcus (1965) derived such an expression for ΔG^*. Figure 4a–c represent some schematic "cartoons" of one-dimensional energy surfaces. Many simplifications are made implicitly in these diagrams. First, a full quantum-mechanical treatment of reaction kinetics requires the calculation of the "Born–Oppenheimer" surface in $N-1$-dimensional space, where N represents the number of all relevant coordinates, orientations, vibrational modes, and so on of the reactants and their surrounding solvent molecules. Here we consider only one general reaction coordinate, labeled as the "solvent reorganization." Second, we assume that the reaction is nonadiabatic, that is, that no mixing between the reactant states and the product states occurs. In this case the intersection of free-energy curves can be derived by straightforward geometry. In adiabatic reactions the free-energy profile between the reactant and product curves in Fig. 4*a–c* would be smoothed and the corresponding barriers lowered. Third, we approximate the free-energy curves by parabola of identical shape. This simplifies the mathematics. On the basis of these assumptions, Fig. 4*a*

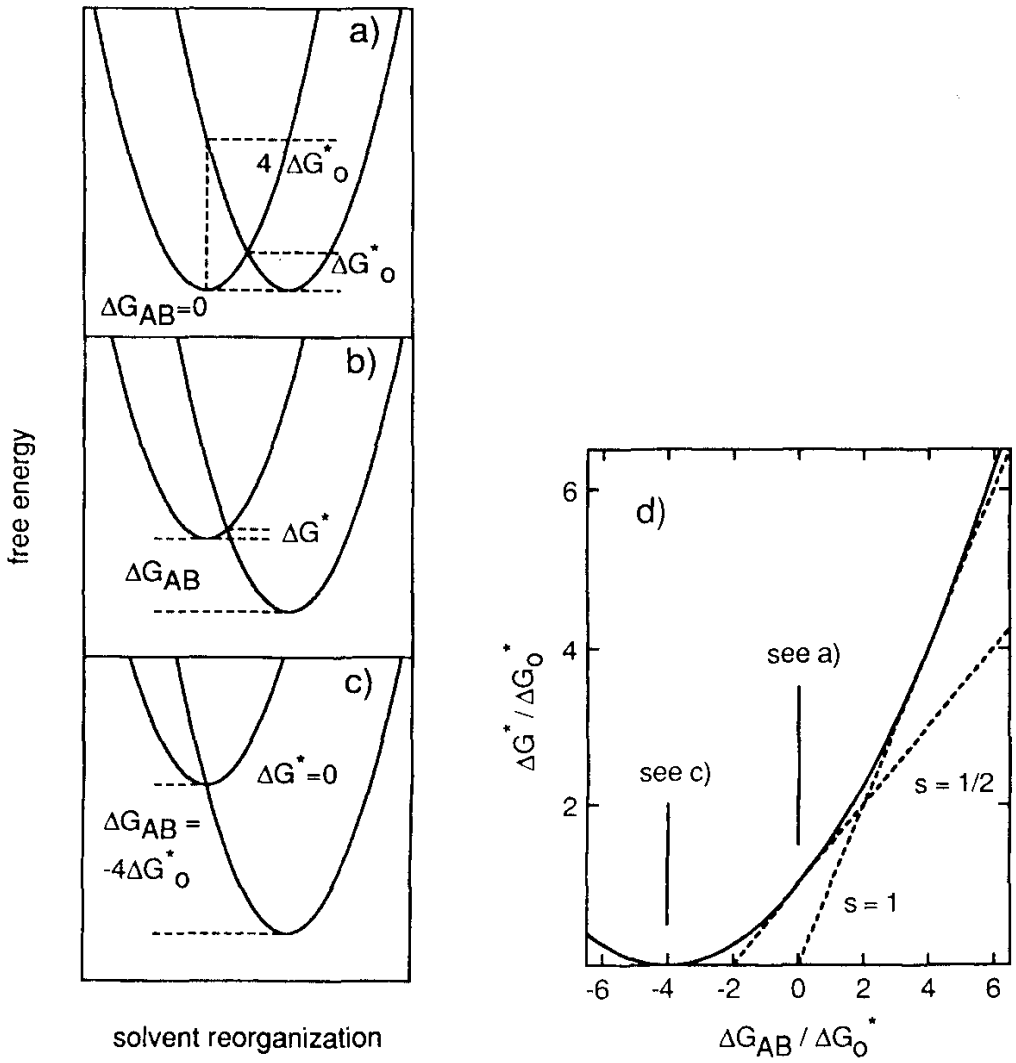

Figure 4 (*a*)–(*d*). Parabolic free-energy curves for outer-sphere electron-transfer reactions. The "general" reaction coordinate represents the reorganization of coordinated water molecules. (*a*) Electron transfer in a system without free-energy change such as reaction 12. In a photochemical reaction without solvent reorganization the energy barrier is $4\Delta G_0^*$. If thermal activation reorganizes the hydration shell, the energy barrier is four times smaller. (*b*) In exergonic reactions ($\Delta G_{AB} < 0$) the reorganization energy ΔG^* is smaller than the "intrinsic barrier" ΔG_0^*. (*c*) Limit of activationless transfer. (*d*) The parabolic Marcus relation (Eq. 13a) in normalized form. The relation describes the dependence of the energy barrier ΔG^* as a function of the free-energy change ΔG_{AB} and the intrinsic barrier ΔG_0^*. The slope is close to unity for very endergonic reactions, approaches 0.5 at $\Delta G_{AB} \sim \Delta G_0^*$, and is zero for activationless transfer (*c*).

represents the situation of a self-exchange reaction such as

$$Fe^{2+} + Fe^{3+} \xrightarrow{k_{11}} Fe^{3+} + Fe^{2+} \qquad (12)$$

The free-energy change between the precursors and the successors of the electron transfer is zero in this case, $\Delta G_{AB} = 0$. If no thermal activation occurs (such as in photochemical reactions), an energy of $4\Delta G_0^*$ is required to bring the system from the left parabola to the product curve one the right-hand side of Fig. 4*a*. If

thermal activation reorganizes the solvent shell, the energy barrier is only ΔG_0^*. Figure 4*b* shows the same parabolic curves for an exergonic reaction, $\Delta G_{AB} < 0$. The reorganization barrier is much smaller in this case. The special case of activationless electron transfer is shown in Fig. 4*c*. In the parabolic model the reorganization energy ΔG^* vanishes if the driving force of the reaction is $\Delta G_{AB} = -4\,\Delta G_0^*$.Based on parabolic reaction diagrams Marcus (1965) derived a relation between the different free energy terms, which can be given in the following form:

$$\Delta G^* = \Delta G_0^* [1 + (\Delta G_{AB}/4\,\Delta G_0^*)]^2 \tag{13a}$$

Figure 4*d* depicts a normalized version of this parabolic function. The calculation of the reorganization energy ΔG^* requires knowledge of the "intrinsic" barrier ΔG_0^*, which can be obtained from self-exchange experiments such as reaction 12. The free-energy change between precursor and successor ΔG_{AB} can often be replaced by the free-energy change of the overall redox step. Linear free-energy plots of $RT \ln k$ versus ΔG_{AB} for a series of reactions with similar 'intrinsic' energy barriers ΔG_0^* will show different slopes; the slope approaches unity for very exergonic reactions in the limit $\Delta G_{AB} = 4\,\Delta G_0^*$. It decreases to 0.5 in the more usual range of near-equilibrium conditions $\Delta G_{AB} \sim \Delta G_0^*$ and is zero for activationless transfer at $\Delta G_{AB} = -4\,\Delta G_0^*$ (Fig. 4*c*). In the "inverted region" beyond this point a decrease in the reaction rates with extremely exergonic potential is predicted. This feature of the Marcus relation as been debated for two decades. Only recently Closs and Miller (1988) presented experimental evidence for an "inverted region" in intramolecular redox kinetics of organic molecules. Transport processes will hide such effects in intermolecular reactions in natural waters. A more intuitive form of Eq. 13a is known as the *Marcus cross-relation*:

$$k_{12} \sim (k_{11} k_{22} K_{12} f_{12})^{1/2} \tag{13b}$$

with

$$\log f_{12} = \frac{(\log K_{12})^2}{\log (k_{11} k_{22}/Z^2)}$$

Here k_{11} and k_{22} are the rate constant for the self-exchange between the reduced and oxidized form of the two reactants and K_{12} refers to the equilibrium constant. This approximation is valid if the work term w in Eq. 11b cancels or can be neglected.

2.4. Comparison of Homogeneous and Heterogeneous Rate Constants

Parsons (1975) used the concept of particle surfaces as electrodes to compare homogeneous and heterogeneous reactions in the marine environment. Two factors are important in this comparison: (1) the change in geometry affects collision frequencies, steric interactions, and so on; and (2) adsorbed species may

react with different activation energy. In gas-phase reactions the geometric effects tend to slow down the reaction rates. At 300 K the surface process occurs at competitive rates only if its activation energy is about 70 kJ mol^{-1} lower than in the homogeneous case (Laidler, 1987). Marcus (1965) compared the bimolecular electron transfer, k_{hom} ($M^{-1}\,s^{-1}$), with the first-order electrochemical reaction k_{het} ($m\,s^{-1}$) on an electrode of surface S:

$$A + B \xrightarrow{k_{hom}} C + D \tag{14}$$

$$A \xrightarrow{k_{het}} C \tag{15}$$

Simple collision theory (see Laidler, 1987) predicts the collision frequencies Z as preexponential factors in Eq. (11b):

$$Z_{hom} = N_A(8\pi kT/m^*)^{1/2}\sigma_{AB}^2 \qquad (\sim 10^{11}\ M^{-1}\,s^{-1}) \tag{16}$$

$$Z_{het} = (kT/2\pi m)^{1/2} \qquad (\sim 10^2\ m\,s^{-1}) \tag{17}$$

where m^* is the reduced mass $m_A m_B/m_A + m_B$. The term in brackets represents the relevant velocity of the species, and σ_{AB} stands for the effective collision cross section. If every collision leads to a reaction and the molecules follow hard-sphere dynamics, the effective cross section approaches $\sigma_{AB} = (r_A + r_B)^2$. Marcus (1965) normalized the rate constants from bimolecular exchange and electrode processes with the above Z values and derived the comparative relation

$$(k_{hom}/Z_{hom})^{1/2} \sim k_{het}/Z_{het} \tag{18}$$

Table 3 confronts measured electrokinetic rate constants k_{het} with values predicted from Eq. 18. The experimental rate constants $k_{hom} = k_{11}$ (see Eq. 12) from bimolecular self-exchange processes between species such as Fe^{3+} and Fe^{2+} were used. The agreement is usually better than a factor of 10 (except for the Co^{3+}/Co^{2+} with its low-spin–high-spin transition). This fair agreement confirms what we would expect: specifically, the activation energy of these os transfer reactions remains unchanged if a reactant is replaced by an electrode. Collision theory approximates the geometric changes correctly.

Not many redox reactions on mineral surfaces follow the two basic assumptions of Eq. 18: outer-sphere transfer and regeneration of the surface during the reaction. Fast reductive dissolutions with powerful reducing agents may potentially lead to an additional test of Eq. 18. In many cases the surface species are consumed during the reaction. Astumian and Schelly (1984) developed a theory to compare a second-order reaction of two reactants in solution (Eq. 14) with a heterogeneous reaction of a dissolved species A and an adsorbed species B. The two different reaction environments are outlined in Figure 5. Here we denote the surface complex as =MO–B:

$$A + {=}MO{-}B \xrightarrow{k_s} C + {=}MO{-}D \tag{19}$$

TABLE 3. Homogeneous Self-Exchange and Electrode Reactions

Redox Couple	k_{hom}[a] $[M^{-1}\,s^{-1}]$	k_{het}(meas.)[b] [cm s^{-1}]	k_{het}(calc.)[c] [cm s^{-1}]
V^{3+}/V^{2+}	1.0×10^{-2}	4.0×10^{-3}	3.2×10^{-3}
Mn^{3+}/Mn^{2+}	3.0×10^{-4}	1.0×10^{-5}	5.5×10^{-4}
Fe^{3+}/Fe^{2+}	4.2	5.0×10^{-3}	6.5×10^{-2}
Co^{3+}/Co^{2+}	3.3	2.0×10^{-7}	5.7×10^{-2}
Cu^{2+}/Cu^{+}	1.0×10^{-5}		1.0×10^{-4}
MnO_4^-/MnO_4^{2-}	7.1×10^{2}	$>10^{-2}$	0.84
O_2/O_2^-	1.0×10^{3}		1.0

[a] Experimental rate constants of homogeneous self-exchange (compare reaction 12). Data from Sutin (1986).
[b] Electrokinetic constants of the reaction at electrode surface [from Marcus (1975); the Mn values are from Parsons (1975)].
[c] Calculated constants for the heterogeneous process using Marcus' theory (Eq. 18). The agreement between theory and experiment is within an order of magnitude. (The deviation of the Co couple has been ascribed to its electronic structure.)

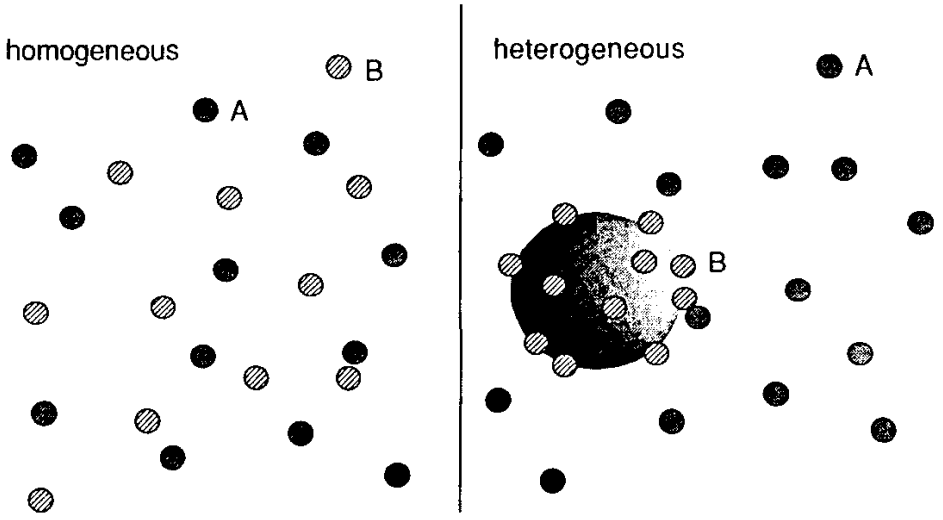

Figure 5. Geometric difference between homogeneous and heterogeneous reactions. The reduction in dimensionality that occurs when the reactants B are all adsorbed to the surface of a mineral particle slows down the reaction rate. This geometric effect is described by Eq. 22 using collision theory.

The authors derived the collision frequency for such a reaction as

$$Z_s = N_A(8kT/\pi m_A)^{1/2} r_P^2 \tag{20}$$

where the velocity is a function of the mass m_A of A, but the effective cross section is determined by the mean radius of the particles, r_p. For the case that the

particles are completely covered with reactants B the relation

$$4\pi r_P^2 N_P = (2r_B)^2 N_B \tag{21}$$

holds, where N_P and N_B refer to the number of particles and species B. Combining the Eqs. 16, 20, and 21, Astumian and Schelly (1984) obtained the ratio

$$k_s/k_{hom} = \pi^{-1}[m_B/(m_A + m_B)]^{1/2}[r_B/(r_A + r_B)]^2 \exp(-\Delta E_a/RT) \tag{22}$$

The first three factors on the right-hand side of this relation are smaller than unity. The reduction in dimensionality that accompanies the transfer of reactant B from solution to an interface slows down the reaction rate. Using realistic values of the masses m_i and the radii r_i, one may predict a maximum estimate of a 50-fold reduction in the rate constant k_s. This geometric "disadvantage" is sometimes compensated by a lower activation energy E_a at the surface. Astumian and Schelly (1984) estimate that E_a of the heterogeneous reaction must be 2.5 to 7.5 kJ mol^{-1} lower to compensate for the geometric effects.

3. APPLICATION: OXYGENATION KINETICS

The oxidation of metal ions by O_2 has been extensively studied because of the relevance of these reactions in geochemical cycles and in water-treatment technology. For different reasons the process lends itself to a conceptual discussion of heterogeneous redox reactions: (1) a large kinetic database of oxygenation kinetics in solution is available (Fallab, 1967; Davison and Seed, 1983; Millero et al., 1987), (2) heterogeneous oxygenation has recently been measured in spectroscopically well-characterized systems (Wehrli and Stumm, 1988), and (3) a report from Taube's group (Stanbury et al., 1980) shows that the oxygenation of Ru(II)–amine complexes follows an outer-sphere mechanism. This opens the perspective to apply Marcus theory to metal oxygenations in solution and at mineral surfaces.

3.1. The Oxygenation of V(IV), Fe(II), Mn(II), and Cu(I)

The reduced species Fe^{2+} and Mn^{2+} have been detected electrochemically in anoxic waters (De Vitre et al., 1988). Vanadyl (VO^{2+}) is known to be incorporated in geoporphyrins in organic-rich sediments (Eckstrom et al., 1983). Moffett and Zika (1988) measured reduced Cu(I) photometrically in surface waters of the open ocean. The oxidation of these four metal species involves a simple one-electron transfer step. Haber and Weiss (1934) proposed a kinetic mechanism for the oxygenation of the ferrous ion, in which the first step in the four-electron reduction of the dioxygen molecule determines the rate. The redox potentials for the corresponding oxygen couples support this view: they are plotted in

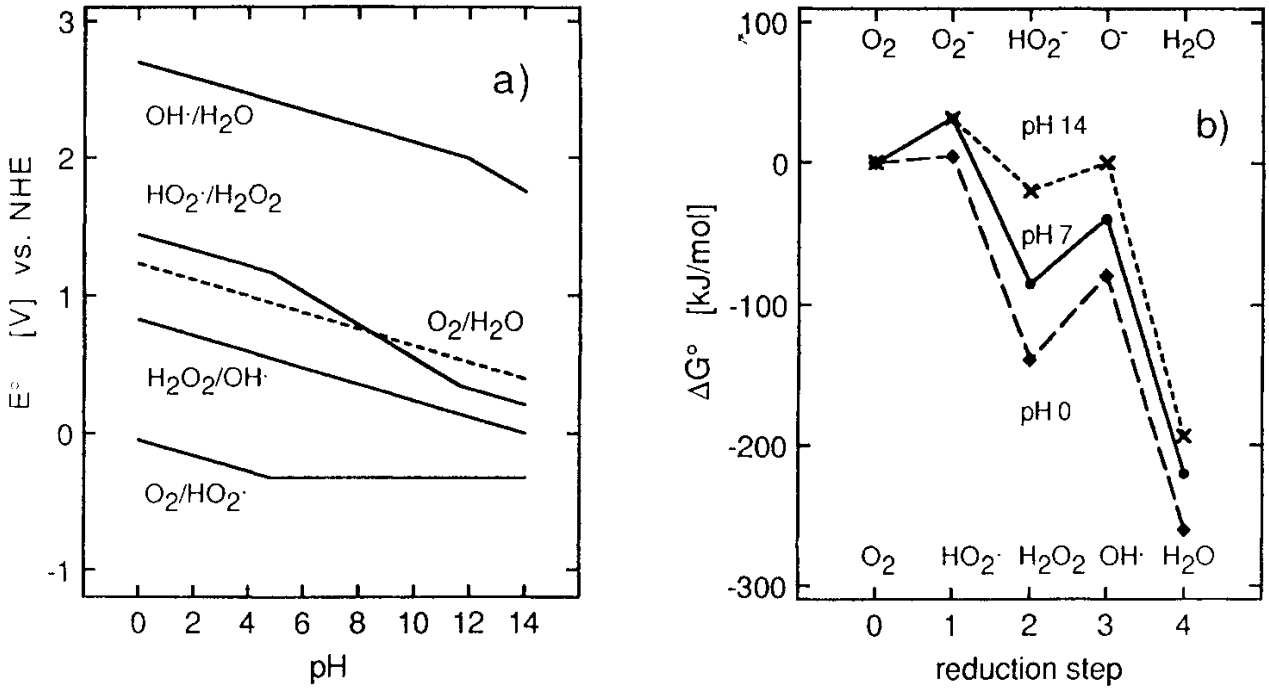

Figure 6. Reduction potentials of the four reduction steps of O_2. (*a*) pH dependence calculated form standard E° data with $p_{O_2} = 1$ atm as reference state and pK values of the intermediates. References: Bielski et al. (1985), Sawyer and Valentine (1981), George (1965). Superoxide is a strong reducing agent. (*b*) Reaction path diagram for the reduction of O_2. The the formation of radicals in the first and third step is endergonic.

Figure 6*a* for the whole pH range. Figure 6*b* presents the four reduction steps in a reaction path diagram that was inspired by Schneider (1988). Both graphs show that the first reduction step form the dioxygen molecule to the superoxide radical is an "uphill" (endergonic) reaction. The superoxide anion (O_2^-) is a powerful reducing agent (Sawyer and Valentine, 1981), which is scavenged in natural systems by a variety of processes including the reduction of Cu(II) and even S_N2-type nucleophilic substitutions on organic compounds.

Several reports confirmed the finding of Stumm and Lee (1961) that the oxidation of Fe(II) by O_2 at neutral pH is accelerated hundredfold if the pH is raised by one unit (Davison and Seed, 1983, Millero et al., 1987). The empirical rate law of the ferrous ion oxygenation at neutral pH is

$$R = -d[Fe^{II}]/dt = k[Fe^{II}][O_2][H^+]^{-2} \qquad (23)$$

Experiments in the acidic pH range are more time-consuming, and kinetic data are quite rare. The work of Singer and Stumm (1970) is in agreement with earlier experiments by Holluta and Kölle (1964), which indicate a change in the pH dependence of the reaction from $\log R \propto [H^+]^{-2}$ to $[H^+]^{-1}$ below pH = 5. The rates approach a pH-independent value below pH 3. Figure 7*a* summarizes the kinetic findings in terms of an observed first-order rate constant k at 25°C and p_{O_2} = 1 atm. This kinetic "titration curve" was plausibly interpreted by Millero

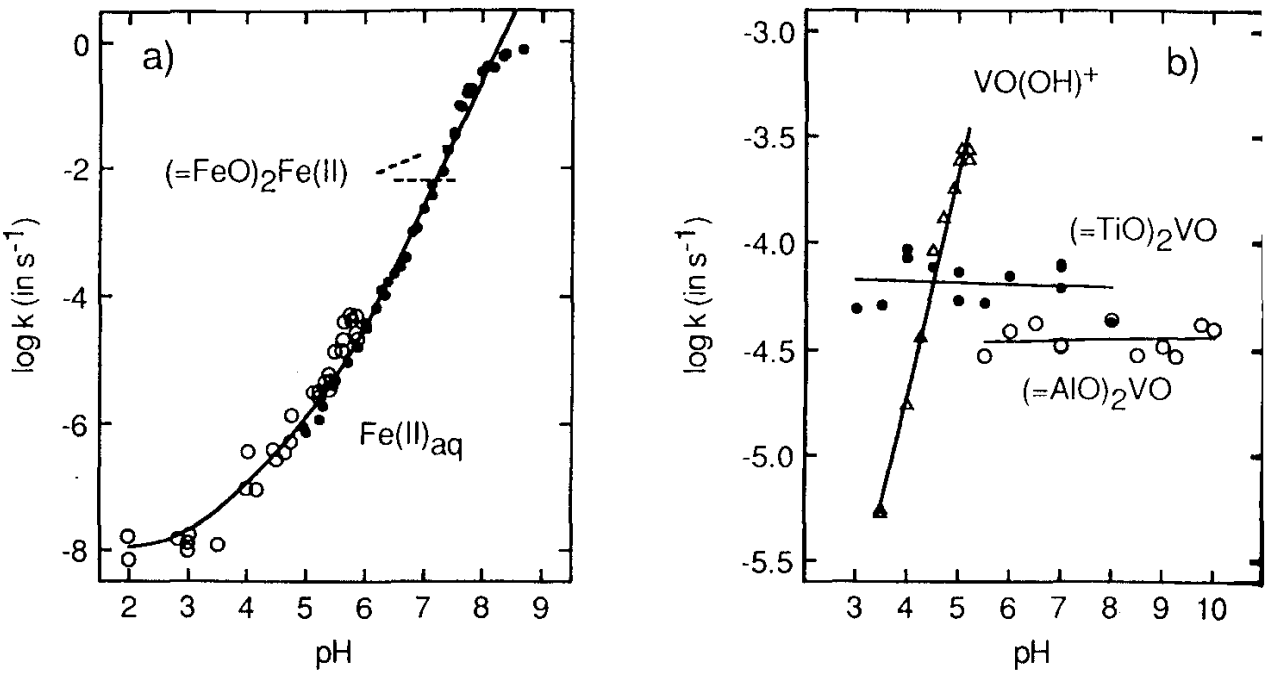

Figure 7. Oxygenation kinetics for 1 atm O_2. (*a*) Oxidation of Fe(II). Open circles represent data by Singer and Stumm (1970), dots are data from Millero et al. (1987). The solid line was calculated with Eq. 26. Small dotted lines represent heterogeneous rate constants for Fe(II) adsorbed to $Fe(OH)_3$ (upper line) and α-FeOOH (lower); data from Tamura et al. (1976). (*b*) Oxygenation of vanadyl in solution and as surface complexes; data from Wehrli and Stumm (1988).

(1985) as a parallel oxidation of the ferrous ion and its hydroxo complexes:

$$\begin{aligned} Fe^{2+} + O_2 &\longrightarrow Fe^{3+} + O_2^- \\ Fe(OH)^+ + O_2 &\longrightarrow Fe(OH)^{2+} + O_2^- \\ Fe(OH)_2 + O_2 &\longrightarrow Fe(OH)_2^+ + O_2^- \end{aligned} \tag{24}$$

Millero (1985) based his kinetic model on the assumption that the first step in the sequential reduction of O_2 to H_2O is rate-limiting. Since the hydrolysis constants of ferrous iron are $pK_1^* = 9.5$ and $p\beta_2^* \approx 20.6$, we may approximate the speciation of Fe(II) in these laboratory experiments the following way:

$$\begin{aligned} [Fe^{2+}] &\approx [Fe^{II}] \\ [Fe(OH)^+] &\approx K_1^*[Fe^{II}]/[H^+] \\ [Fe(OH)_2] &\approx \beta_2^*[Fe^{II}]/[H^+]^2 \end{aligned} \tag{25}$$

The pseudo-first-order rate law for excess dissolved oxygen can then be given as the sum of the three parallel oxidation pathways:

$$\begin{aligned} R &= k_0[Fe^{2+}] + k_1[Fe(OH)^+] + k_2[Fe(OH)_2] \\ &= \{k_0 + k_1 K_1^*/[H^+] + k_2\beta_2^*/[H^+]^2\}[Fe^{II}] \\ &= k[Fe^{II}] \end{aligned} \tag{26}$$

The solid line in Fig. 7*a* was calculated according to Eq. 26 with the constants $k_0 = 1.0 \times 10^{-8}$, $k_1 = 3.2 \times 10^{-2}$ and $k_2 = 1.0 \times 10^4$ (s^{-1}) for 1 atm partial pressure of oxygen. The corresponding second-order rate constants $k_i' = k_i / K_H$ are given in Table 4. (The Henry's law constant for oxygen at 25°C is $K_H = 1.26 \times 10^{-3}$ M atm^{-1}.)

The empirical rate law in Eq. 23 holds only for the initial rates. Tamura et al. (1976) observed an autocatalytic effect of the ferric precipitates produced in the reaction. Sung and Morgan (1980) identified γ-FeOOH as the primary oxidation product at neutral pH and confirmed its autocatalytic effect. Adsorbed Fe(II) seems to compete in an additional parallel reaction with the dissolved ferrous species. Fast surface reaction rates resulted from a fit of the kinetic data. Examples of these constants are included in Fig. 7*a* for comparison. They represent only estimates of an order of magnitude because Tamura et al. (1976) did not determine the surface concentration of Fe(II). However, Figure 2 shows qualitatively that the ferrous ion is adsorbed specifically to mineral surfaces.

TABLE 4. Thermodynamics and Kinetics of Metal-Ion Oxygenation[a]

Redox Couple	log β_i[b] (ox)	(red)	E°[c] (V)	log K[d] First Step	log k' (M^{-1} s^{-1})	Reference[e]
O_2/O_2^-			−0.16			1
O_2/HO_2			0.12			1
Fe^{3+}/Fe^{2+}			0.771	−15.7	−5.1	2
$Fe(OH)^{2+}/Fe(OH)^+$	−2.19	−9.50	0.34	−8.45	1.4	2
$Fe(OH)_2^+/Fe(OH)_2$	−5.70	−20.6	−0.02	−3.04	6.9	3
$(\equiv FeO)_2Fe^+/(\equiv FeO)_2Fe$					0.7	4
Cu^{2+}/Cu^+			0.159	−5.41	4.3	5
$CuCl^+/CuCl$	0.4	3.1	0.32	−8.11	2.9	5
VO_2^+/VO^{2+}			1.000		< −5	6
$VO_2^+/VO(OH)^+$		−5.8	0.72	−10.1	0.02	6
$(\equiv AlO)_2VO^+/(\equiv AlO)_2VO$					−1.6	6
$(\equiv TiO)_2VO^+/(\equiv TiO)_2VO$					−1.3	6
$(\equiv FeO)_2Mn^+/(\equiv FeO)_2Mn$					−0.16	7
$(\equiv AlO)_2Mn^+/(\equiv AlO)_2Mn$					−1.55	7

[a] Figure 8 plots the linear free-energy relation between log K of the equilibrium $M_{red} + O_2 \Leftrightarrow M_{ox} + O_2^-$ and log k from experimental oxygenation rates.

[b] Stability constants of the oxidized (ox) and reduced (red) species from Smith and Martell (1979) except for CuCl (Ref. 5).

[c] The E° values of the aquo complexes were taken from Bard et al. (1985). Reduction potentials of the hydroxo and chloro complexes were calculated from the listed stability constants.

[d] Equilibrium constants were calculated from the reduction potentials of the metal and oxygen couples using $\log K = \Delta E^{\circ}/0.059$. The assumed product was O_2^- in the case of Fe and Cu and HO_2 in the case of vanadyl (see text).

[e] References: (1) Sawyer and Valentine (1981) for 1 M O_2 as standard state. (2) calculated from Singer and Stumm (1970); (3) Millero et al. (1987); (4) estimated value for goethite from Tamura et al. (1976); (5) Sharma and Millero (1988). (6) Wehrli and Stumm (1988), (7) Davies and Morgan (1989).

Vanadyl (VO^{2+}) is an ideal cation for the study of heterogeneous oxidations for several reasons: (1) the electron-transfer behavior of VO^{2+} is in many aspects similar to that of Fe^{2+} (Rosseinsky, 1972, Wehrli et al., in press), (2) the experimental conditions can be chosen so that vanadyl is completely adsorbed at pH > 4 (Fig. 2), (3) the adsorbed V(IV) species have been characterized by ENDOR spectroscopy as inner-sphere surface complexes $(\equiv MO)_x VO$ (Motschi and Rudin, 1984). Adsorption experiments are compatible with $x = 2$. The oxygenation rates of VO^{2+} adsorbed to anatase and δ-Al_2O_3 follow the empirical rate law

$$-d\{(\equiv MO)_2VO\}/dt = k'\{(\equiv MO)_2VO\} \cdot [O_2] \tag{27}$$

where { } represent surface concentrations in moles per square meter (Wehrli and Stumm, 1989).

The rates are independent of pH, which suggests that the solution composition exerts only negligible effects on the speciation of adsorbed vanadyl. The oxygenation rate of dissolved V(IV), on the other hand, increases by an order of magnitude as the pH is increased by one unit. This observation indicates that the hydroxo complex $VO(OH)^+$ acts as the precursor of the oxidation step. Figure 7*b* compares the pseudo-first-order rate constants of the homogeneous and the heterogeneous reaction at 25°C and $p_{O_2} = 1$ atm. Geometric effects of the reduction in dimensionality as summarized in Eq. 22 slow down the heterogeneous rate constant. These effects can be taken into account as follows. If we insert the relative molar mass of vanadyl and dioxygen and a radius $r_A = 0.12$ mm for O_2 and $r_B = 0.4$ mm for $VO(OH)^+_{aq}$ into Eq (22), we estimate a ratio $k_s/k_{hom} = 0.17$ or a sixfold decrease in the rate of the surface reaction due the geometric effect. We may therefore compensate the geometric slowing down by calculating a corrected surface rate constant $k_s^c \sim 6k_s$. The resulting rate constants of dissolved and adsorbed vanadyl are remarkably similar:

$$\begin{aligned}
&VO(OH)^+ + O_2 \xrightarrow{k'} k' = 1.07 \qquad (M^{-1}\,s^{-1}) \\
&(\equiv TiO)_2VO + O_2 \xrightarrow{k'_s} k'_s = 0.052; \quad k_s^c = 0.31 \qquad (M^{-1}\,s^{-1}) \\
&(\equiv AlO)_2VO + O_2 \xrightarrow{k'_s} k'_s = 0.028; \quad k_s^c = 0.17 \qquad (M^{-1}\,s^{-1})
\end{aligned} \tag{28}$$

These corrected values correspond to an oxygenation of surface complexes extrapolated to a bimolecular reaction in solution. The close agreement in the oxygenation kinetics of dissolved $VO(OH)^+$ and with that of the surface complexes $(\equiv MO)_2VO$ supports the evidence for inner-sphere surface coordination from spectroscopic and thermodynamic experiments.

The one-electron redox couples Mn^{2+}/Mn^{3+} and Cu^+/Cu^{2+} complete the emerging picture of metal oxygenations: Cu^+ shows low affinity for surfaces, and

its oxidation occurs predominantly in solution. The oxidation of Mn(II), on the other hand, has so far been quantified only for surface complexes. The extremely slow reaction of dissolved Mn^{2+} (Diem and Stumm, 1984) (see Fig. 1*a*) may be a consequence of the prohibitive thermodynamics of the first electron-transfer step

$$Mn^{2+} + O_2 \Leftrightarrow Mn^{3+} + O_2^-, \qquad \Delta G^\circ = +177 \text{ kJ mol}^{-1} \tag{29}$$

which results from the high reduction potential of $E^\circ = 1.5$ V for the Mn(III)/Mn(II) couple and the positive free energy of formation for the superoxide radical ($\Delta G^\circ \sim 31.9$ kJ mol^{-1}). Solid surfaces, however, seem to stabilize the products of reaction 29. Davies and Morgan (1989) found a kinetic behavior of adsorbed Mn(II) that is in line with the findings for vanadyl. The data are listed in Table 4 for comparison. The authors described the heterogeneous rate law as

$$-d[Mn^{II}]/dt = k_s' <(=MO)_2Mn> A[O_2] \tag{30}$$

where $< >$ stands for the surface concentration in moles per gram of solid and A represents the solids concentration in grams per liter. Manganese was only partially adsorbed in these experiments. An increase in the solids concentration accelerates the reaction rate. The above rate law collapses to a form such as Eq. 27 in the limiting case of complete adsorption.

The oxygenation kinetics of Cu(I) in different electrolyte solutions has been measured by Sharma and Millero (1988). Contrary to Fe(II) and V(IV), the rates were found to be independent of $[H^+]$ in the range $5.3 < pH < 8.6$. The chloride ion, however, exerts a strong inhibitory effect. Millero (1985) interpreted the observations with a similar pseudo-first-order rate law as in the case of ferrous iron. In presence of excess oxygen the rate is given as

$$-d[Cu^I]/dt = k_0[Cu^+] + k_1[CuCl] + k_2[CuCl_2^-] + k_3[CuCl_3^{2-}] \tag{31}$$

Sharma and Millero (1988) determined the corresponding second-order rate constants $k_0' = 2.1\ 10^4$ and $K_1' = 8.7\ 10^2\ M^{-1}\ s^{-1}$ in sea water. The di and trichlorocomplexes were not sufficiently reactive to produce detectable rate constants. Thus the chloride ion, which stabilizes the soft reactant Cu(I) inhibits the oxygenation, whereas OH^-, which stabilizes the product Fe(III), accelerates the rate of Fe(II) oxidation. The reaction of Cu(I) with O_2 represents an interesting test case because the reverse reaction has been measured by pulse radiolysis. We may therefore apply the principle of microscopic reversibility to the electron-transfer step:

$$Cu^+ + O_2 \underset{k_-}{\overset{k_+}{\Leftrightarrow}} Cu^{2+} + O_2^- \tag{32}$$

where k_+ was given above as k_0'. The review of Bielski et al. (1985) lists k_- $8 \times 10^9\ M^{-1}\ s^{-1}$. From $K = k_+/k_-$ we obtain the kinetic estimate of

$\Delta G^\circ = 31.9\ \text{kJ mol}^{-1}$ for reaction 32. This value should be compared to the thermodynamic redox potentials for the process with 1 M O_2 as the standard state. The relevant redox potentials are 0.158 and -0.16 V for the reduction of Cu(II) and O_2 (Sawyer and Valentine, 1981), respectively. From these thermodynamic data we calculate $\Delta G^\circ = -nFE^\circ = 30.7\ \text{kJ mol}^{-1}$. The close agreement indicates that the redox kinetics of copper in natural waters is, indeed, governed by reaction 32 as the rate-limiting step.

3.2. Outer-Sphere Reduction of Molecular Oxygen

The distinction between inner- and outer-sphere oxygenation evokes the question: "Does the dioxygen molecule enter the coordination sphere of the metal complex?" An inner-sphere reduction of O_2 would therefore involve a dioxygen complex as precursor and a coordinated superoxide radical in the successor complex. It should be possible to detect metal-bound superoxide by ESR spectroscopy. For an os reaction, on the other hand, only the encounter complex forms. The coordination shell of the metal center remains unchanged. Because of the transient nature of the os species, such mechanisms are difficult to prove directly. An indirect approach exploits the linear free-energy relation (LFER) based on Eq. 13. Because the rate-limiting step in the reduction of oxygen is endergonic (Fig. 7*b*) we expect a slope of a LFE plot log k versus log K of unity in the case that the "intrinsic" exchange barrier is smaller than the free energy of activation: $\Delta G_0^* < \Delta G^*$ (see Eq. 13a and Fig. 4*d*). The relevant redox potentials for the reactions discussed in the previous section were calculated from standard redox potentials (Bard et al., 1985) and the available complex formation constants (Smith and Martell, 1979). Based on the reversible equilibrium in reaction 32, the author assumes that the O_2/O_2^- couple determines the rate-limiting step. The only exception is vanadyl. The hypothetical product of reaction 33, $V^{V}O(OH)^{2+}$, would be very acidic. A protonation constant of VO_2^+ is not known. The relevant redox potential is therefore estimated from reaction 34:

$$V^{IV}O(OH)^+ + O_2 \longrightarrow V^{V}O(OH)^{2+} + O_2^- \qquad (33)$$

$$VO(OH)^+ + O_2 \longrightarrow VO_2^+ + HO_2 \qquad (34)$$

The thermodynamic and kinetic data are summarized in Table 4. The equilibrium constants as listed in Table 4 are calculated from $\log K = \Delta E^\circ/0.059$ and $\Delta E^\circ = -E^\circ_{(M)} + E^\circ_{(O_2)}$ and involve the standard reduction potentials of the metal couple and of oxygen at $[O_2] = 1\ M$. This standard state is more suitable for kinetic calculations than the more widely used convention $p_{O_2} = 1$ atm. The calculation of *thermodynamic* equilibrium constants for the surface complexes is more difficult (Sposito, 1983) and requires further work. Figure 8 displays the resulting LFER. A theoretical line of slope one fits the data over a broad range of 13 $\log k'$ units. This analysis supports an outer-sphere mechanism for the

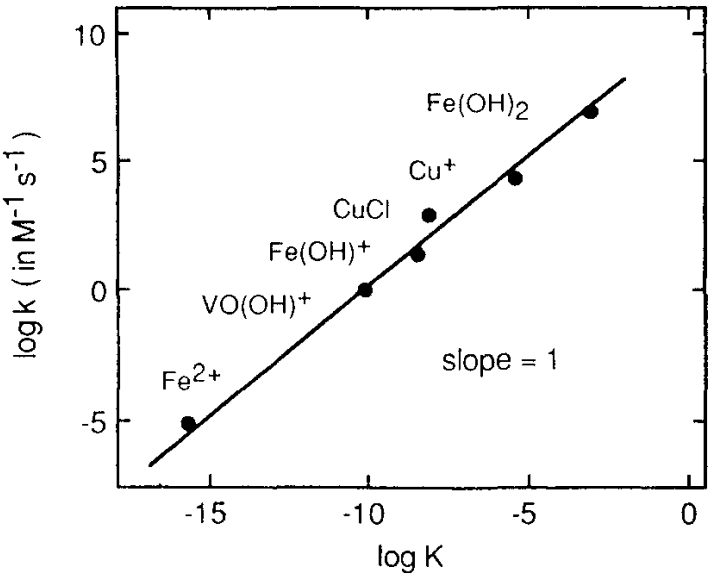

Figure 8. Linear free-energy relation for the oxygenation of metal ions. Data are listed in Table 4. The slope of unity is predicted by Marcus theory for endergonic outer-sphere electron-transfer steps.

oxygenation of V(IV), Fe(II), and Cu(I). Stanbury et al. (1980) derived a similar result for Ru(II)–amine complexes. They found a slope of $\frac{1}{2}$, which may indicate that the intrinsic barrier in Eq. 13a is approximately $\Delta G_0^* \approx \Delta G^*$ in this case. This group also published the first estimate of the self-exchange rate of the O_2/O_2^- couple, which is listed in Table 3. If the oxidation of Fe^{2+} occurs by an outer-sphere mechanism, then the kinetic observations of Singer and Stumm (1970) can be predicted from the self-exchange rates of the reactants. Application of the Marcus cross-relation (Eq. 13b) to the data of the self-exchange constants for iron and oxygen in Table 3 yields the prediction $k'_0(\text{calc.}) = 1.6 \times 10^{-5}$, which agrees well with the observed value $k'_0 = 1.0 \times 10^{-5}\ M^{-1}\,s^{-1}$.

The three metal centers that follow the LFER for outer-sphere electron transfer in Figure 8 share a common aspect of their electronic structure. In the oxidation of d^1-V(IV), d^6-Fe(II), and d^{10}-Cu(I) an electron from a t_{2g} or a t_2 orbital is removed. Luther (Chapter 6, this volume) shows that these orbitals with π symmetry may overlap with the antibonding π^* orbital of O_2 in an encounter complex. In d^5-Mn(II), however, the leaving electron occupies an e_g orbital that points toward the coordinated ligands. The Mn(II) center is therefore a candidate for an inner-sphere electron transfer as proposed by Davies and Morgan 1989).

3.3. Kinetic Estimate for the Redox Potential of Adsorbed Metal Ions

Thermodynamic parameters such as the redox potential are difficult to measure for discrete surface species at the mineral–water interface. If the surface complexes are also oxidized by an os mechanism, we may use the LFER in Figure 8 to estimate E^0 from observed rate constants. The LFER plot translates

to the numerical relation

$$\log k' = \log k'(0) + \Delta E^\circ / 0.059 \tag{35}$$

with the intercept at zero potential of $\log k'(0) = 10.2\,(k/M^{-1}\,s^{-1})$, which is quite close to the theoretical limit of $\log k' = 11.0$ from Eq. 16. In order to compare the heterogeneous rate cc nstants with those measured in solution, we correct for the reduction in dimensionality according to the approximation derived from Eq. 22 and use $k_s^c \sim 6k_s'$. Applying the LFER in Eq. 35 to the oxygenation rates of vanadyl on anatase and of Fe(II) on goethite form Table 4, we calculate

$$\begin{aligned} (\equiv FeO)_2Fe^+ + e^- &\Leftrightarrow (\equiv FeO)_2Fe^{II} \qquad (E^\circ = 0.36\ V) \\ (\equiv TiO)_2VO^+ + e^- &\Leftrightarrow (\equiv TiO)_2V^{IV}O \qquad (E^\circ = 0.73\ V) \end{aligned} \tag{36}$$

These estimates are close to the reduction potentials for the monohydroxo complexes: $E^\circ = 0.34$ and 0.72 V for Fe(II) and V(IV), respectively. If we apply the procedure to the manganese data of Davies and Morgan (1989), we obtain an estimate of $E^\circ = 0.41$ V for the surface complex on goethite that contrasts with the value of $E^\circ = 0.9$ V for the couple $MnOH^{2+}/MnOH^+$. This large discrepancy in the case of Mn(II) is indirect evidence for an inner-sphere oxygenation of the Mn(II) surface complex. Thermodynamic and kinetic approaches are possible to test the extrapolation of redox potentials of surface species with the help of the LFER in Eq. 35: a thermodynamic calculation of E° may be based on the adsorption equilibria of the oxidized and reduced species. Kinetic measurements of other os redox processes may verify (or falsify) the estimates. The characterization of the reducing or oxidizing power of mineral surface species remains a challenge.

3.4. Half-Life Values in Natural Waters

A tentative answer to the question "What benefit may environmental science gain from such mechanistic arguments?" is given in Figure 9. The oxygenation kinetics of reduced metal centers in air-saturated waters vary over many orders of magnitude depending on (1) the redox potential of the aqueous metal couple and (2) the coordinated ligands. The large difference in the half-life of the aquo ions of Fe(II) and Cu(I) illustrates this point; the half-life of the weaker reducing agent Fe^{2+} is in the order of 10 years, while Cu^+ is oxidized within seconds. Coordinated oxygen donors drastically change the reduction potential. Two OH^- groups bound to Fe(II) shift its redox potential by ~ 0.77 V. As a consequence, the half-life of the Fe(II) species changes by 12 orders of magnitude or from 10 yr to less than 1 ms. Adsorption acts like hydrolysis: the two-dimensional array of oxygen donor ligands at mineral surfaces (Fig. 3) binds adsorbed metals in an inner-sphere coordination. Our kinetic analysis has shown that adsorption induces a change in redox potential that is similar to the effect of one coordinated OH^-. As a consequence surface complexes of Fe(II) and V(IV)

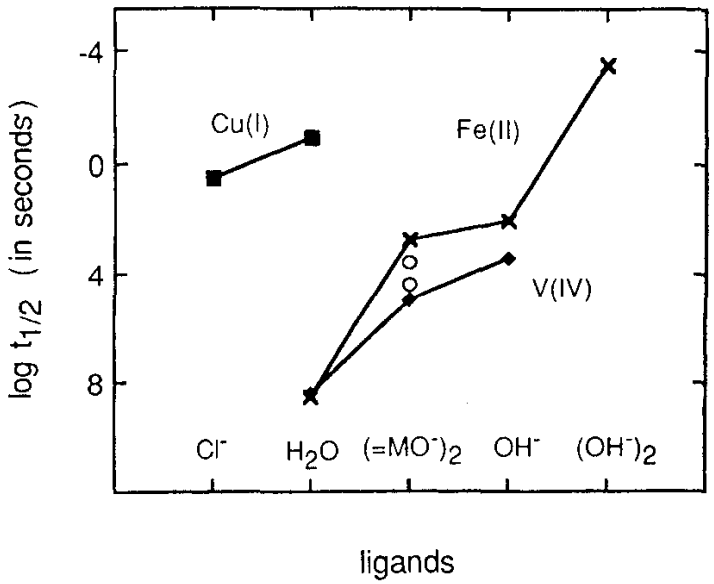

Figure 9. Half-life of metal complexes at $p_{O_2} = 0.21$. Fe(II) spans a range of 10 years to milliseconds. The surface complexes with the ligands $=MO^-$ show a reactivity similar to monohydroxo complexes in solution. Open circles represent Mn(II).

exhibit a half-life close to that of the monohydroxo complexes. If the change in redox potential on adsorption can be veryfied independently, the simple relation between E° and log k in Figure 8 will allow us to treat surface oxygenation just like an electrode reaction.

It was the goal of this kinetic analysis to distinguish between the individual reactivities of different metal species. Only a mechanistic understanding at the molecular level allows us to find predictive correlations such as Eq. 35. In our heterogeneous environment, however, we face a massive parallelism in reaction rates. Within the kinetic framework of Hoigné's chapter (Chapter 2, this volume), the individual reactivities can be aggregated into "environmental factors," which allow the quantitative assessment of reaction rates measured in the field.

Acknowledgment

I thank Werner Stumm, Walter Schneider, and James J. Morgan. Their advice, support, and encouragement in front of different activation barriers made this journey into the world of rust and heterogeneity possible. A nice linear free-energy plot by René Schwarzenbach convinced me to calculate Figure 8.

REFERENCES

Astumian, R. D., and Z. A. Schelly (1984), "Geometric Effects of Reduction of Dimensionality in Interfacial Reactions," *J. Am. Chem. Soc.* **106**, 304 308.

Bard, A. J., R. Parsons, and J. Jordan (1985), *Standard Potentials in Aqueous Solutions*, IUPAC, Dekker, New York, p. 834.

Bielski, B. H. J., D. E. Cabelli, and R. L. Arudi (1985), "Reactivity of HO_2/O_2^- Radicals in Aqueous Solution," *J. Phys. Chem. Ref. Data.* **14**, 1041–1100.

Closs, G. L. and J. R. Miller (1988), "Intramolecular Long-Distance Electron Transfer in Organic Molecules," *Science* **240**, 440–447.

Combes, J. M. (1989), Ph.D. thesis, University of Paris, p. 7.

Crowther, D. L., J. G. Dillard, and J. W. Murray (1983), "The Mechanism of Co(II) Oxidation on Synthetic Birnessite," *Geochim. Cosmochim. Acta.* **47**, 1399–1403.

Davies, S. H. R., and J. J. Morgan (1989), "Manganese(II) Oxidation Kinetics on Oxide Surfaces," *J. Colloid. Interface Sci.* **129**, 63–77.

Davison, W. (1985), "Conceptual Models for Transport at a Redox Boundary," in W. Stumm, Ed., *Chemical Processes in Lakes*, Wiley-Interscience, New York, pp. 31–53.

Davison, W. and G. Seed (1983), "The Kinetics of the Oxidation of Ferrous Iron in Synthetic and Natural Waters," *Geochim. Cosmochim. Acta.* **47**, 67–79.

De Vitre, R. R., J. Buffle, D. Perret, and R. Baudat (1988), "A Study of Iron and Managanese Transformations at the O_2/S(-II) Transition Layer in a Eutrophic Lake (Lake Bret, Switzerland): A Multimethod Approach," *Geochim. Cosmochim. Acta.* **52**, 1601–1613.

Diem, D. and W. Stumm (1984), "Is Dissolved Mn^{2+} Being Oxidized by O_2 in Absence of Mn-bacteria or Surface Catalysts?," *Geochim. Cosmochim. Acta.* **48**, 1571–1573.

Dillard, J. G., and C. V. Schenk (1986), "Interaction of Co(II) and Co(III) Complexes on Synthetic Birnessite: Surface Characterization," in J. A. Davis and K. F. Hayes, Eds., *Geochemical Processes at Mineral Surfaces*, American Chemical Society, Washington DC, pp. 503–522.

Eckstrom, A., C. J. R. Fooks, T. Hambley, H. J. Loeh, S. A. Miller, and J. C. Taylor (1983), "Determination of the Crystal Structure of a Porphyrine Isolated from Oil Shale," *Nature* **306**, 173–174.

Fallab, S. (1967), "Reactions with Molecular Oxygen," *Angew. Chem., Int. Ed.* **6**, 496–507.

Garrels, R. M., F. T. Mackenzie, and C. Hunt (1973), *Chemical Cycles and the Global Environment*, William Kaufmann, Los Altos, CA.

George, P. (1965), "The Fitness of Oxygen," in T. E. King, H. S. Mason, and M. Morrison, Eds., *Oxidases and Related Redox Systems*, Wiley, New York, pp. 3–36.

Gordon, G., and H. Taube (1962), "Oxygen Tracer Experiments on the Oxidation of Aqueous Uranium(IV) with Oxygen-Containing Oxidizing Agents," *Inorg. Chem.* **1**, 69–75.

Haber, F., and J. Weiss (1934), "The Catalytic Decomposition of Hydrogen Peroxide by Iron Salts," *Proc. Royal Soc. (London)* **A147**, 332–351.

Haim, A. (1983), "Mechanisms of Electron Transfer Reactions: The Bridged Activated Complex," *Progr. Inorg. Chem.* **30**, 273–357.

Holluta, J., and W. Kölle (1964), "Über die Oxydation von zweiwertigem Eisen durch Luftsauerstoff," *Das Gas- und Wasserfach.* **105**, 471–474.

Koch, D. F. A. (1957), "Kinetics of the Reaction between Manganese Dioxide and Ferrous Iron," *Aust. J. Chem.* **10**, 150–159.

Laidler, K. J. (1987), *Chemical Kinetics*, Harper, New York.

Lowson, R. T. (1982), "Aqueous Oxidation of Pyrite by Molecular Oxygen," *Chem. Rev.* **82**, 461–497.

Marcus, R. A. (1965), "On the Theory of Electron-Transfer Reactions. VI Unified Treatment for Homogeneous and Electrode Reactions," *J. Chem. Phys.* **43**, 679–701.

Marcus, R. A. (1975), "Electron Transfer in Homogeneous and Heterogeneous Systems," in E. D. Goldberg, Ed., *The Nature of Seawater*, Dahlem Konferenzen, Berlin, pp. 477–503.

Millero, F. (1985), "The Effect of Ionic Interactions on the Oxidation of Metals in Natural Waters," *Geochim. Cosmochim. Acta* **49**, 547–554.

Millero, F. J., S. Sotolongo, and M. Izaguirre (1987), "The Oxidation Kinetics of Fe(II) in Seawater," *Geochim. Cosmochim. Acta* **51**, 793–801.

Moffett, J. W., and R. G. Zika (1988), "Measurement of Copper(I) in Surface Waters of the Subtropical Atlantic and Gulf of Mexico," *Geochim. Cosmochim. Acta* **52**, 1849–1857.

Motschi, H., and M. Rudin (1984), "^{27}Al ENDOR Study of VO^{2+} Adsorbed on δ-Alumina," *Colloid Polym. Sci.* **262**, 579–583.

Oscarson, D. W., P. M. Huang, C. Defosse, and A. Herbillon (1981), "Oxidative Power of Mn(IV) and Fe(III) Oxides with Respect to As(III) in Terrestrial and Aquatic Environments," *Nature* **291**, 50–51.

Parsons, R. (1975), "The Role of Oxygen in Redox Processes in Aqueous Solution," in E. D. Goldberg, Ed., *The Nature of Sea Water*, Dahlem Konferenzen, Berlin, pp. 505–522.

Rapsomanikis, S., and J. H. Weber (1985), "Environmental Implications of Methylation of Tin(II) and Methyltin(IV) Ions in the Presence of Manganese Dioxide," *Environ. Sci. Technol.* **19**, 352–356.

Rosseinsky, D. R. (1972), "Aqueous Electron-Transfer Reactions. Vanadium(IV) as Reductant Compared with Iron(II)," *Chem. Rev.* **72**, 215–229.

Rudin, M., and H. Motschi (1984), "A Molecular Model for the Structure of Copper Complexes on Hydrous Oxide Surfaces: An ENDOR Study of Ternary Cu(II) Complexes on δ-Alumina," *J. Colloid Interface Sci.* **98**, 385–393.

Sawyer, D. T., and J. S. Valentine (1981), "How Super is Superoxide?" *Acc. Chem. Res.* **14**, 393–400.

Schindler, P. W., and W. Stumm (1987), "The Surface Chemistry of Oxides, Hydroxides and Oxide Minerals," in W. Stumm, Ed., *Aquatic Surface Chemistry*, Wiley-Interscience, New York, pp. 83–110.

Schneider, W. (1988), "Iron Hydrolysis and the Biochemistry of Iron—The Interplay of Hydroxide and Biogenic Ligands," *Chimia* **42**, 9–20.

Segal, M. G., and R. M. Sellers (1984), "Redox Reactions at Solid–Liquid Interfaces," *Adv. Inorg. Bioinorg. Mech.* **3**, 97–129.

Sharma, V. K., and F. J. Millero (1988), "Effect of Ionic Interactions on the Rates of Oxidation of Cu(I) with O_2 in Natural Waters," *Mar. Chem.* **25**, 141–161.

Silverman, J., and R. W. Dodson (1952), "The Exchange Reaction between the Two Oxidation States of Iron in Acid Solution," *J. Phys. Chem.* **56**, 846–852.

Singer, P. C., and W. Stumm (1970), "Acidic Mine Drainage: The Rate-Determining Step," *Science* **167**, 1121–1123.

Smith, R. M., and A. E. Martell (1979), *Critical Stability Constants*, Plenum Press, New York.

Sposito, G. (1983), "On the Surface Complexation Model of the Oxide–Aqueous Solution Interface," *J. Colloid Interface Sci.* **91**, 329–340.

Stanbury, D. M., O. Haas, and H. Taube (1980), "Reduction of Oxygen by Ruthenium(II) Ammines," *Inorg. Chem.* **19**, 518–524.

Stone, A. T. (1986), "Adsorption of Organic Reductants and Subsequent Electron Transfer on Metal Oxide Surfaces," in J. A. Davis and K. F. Davis and K. F. Hayes, Eds., *Geochemical Processes at Mineral Surfaces*, American Chemical Society, Washington DC, pp. 446–461.

Stone, A. T., and J. J. Morgan (1987), "Reductive Dissolution of Metal Oxides," in W. Stumm, Ed., *Aquatic Surface Chemistry*, Wiley-Interscience, New York, pp. 221–254.

Stumm, W. (1978), "What is the $p\varepsilon$ of the Sea?," *Thalassia Jugoslavica* **14**, 197–208.

Stumm, W., and G. F. Lee (1961), "Oxygenation of Ferrous Iron," *Indust. Eng. Chem.* **53**, 143–146.

Sung, W., and J. J. Morgan (1980), "Kinetics and Product of Ferrous Iron Oxygenation in Aqueous Systems," *Environ. Sci. Technol.* **14**, 561–567.

Sutin, N. (1986), "Theory of Electron Transfer," in J. J. Zuckerman, Ed., *Inorganic Reactions and Methods*, VCH, Weinheim, pp. 16–46.

Tamura, H., K. Goto, and M. Nagayama (1976), "The Effect of Ferric Hydroxide on the Oxygenation of Ferrous Ions in Neutral Solutions," *Corrosion Sci.* **16**, 197–207.

Van der Weijden, C. H., and M. Reith (1982), "Chromium(III)–Chromium(VI) Interconversions in Seawater," *Mar. Chem.* **11**, 565–572.

Voudrias, E. A., and M. Reinhard (1986), "Abiotic Organic Reactions at Mineral Surfaces," in J. A. Davis and K. F. Hayes, Eds., *Geochemical Processes at Mineral Surfaces*, American Chemical Society, Washington DC, pp. 462–486.

Wehrli, B., and W. Stumm (1988), "Oxygenation of Vanadyl(IV). Effect of Coordinated Surface Hydroxyl Groups and OH^-," *Langmuir* **4**, 753–758.

Wehrli, B., and W. Stumm (1989), "Vanadyl in Natural Waters: Adsorption and Hydrolysis Promote Oxygenation," *Geochim. Cosmochim. Acta* **53**, 69–77.

Wehrli, B., B. Sulzberger, and W. Stumm, "Redox Processes Catalyzed by Hydrous Oxide Surfaces," *Chem. Geol.* (in press)

Yasunaga, T. and T. Ikeda (1986), "Adsorption–Desorption Kinetics at the Metal-oxide–Solution Interface studied by Relaxation Methods," in J. A. Davies and K. F. Hayes, Eds., *Geochemical Processes at Mineral Surfaces*, American Chemical Society, Washington, DC, pp. 230–253.

Zabin, B. A., and H. Taube (1964), "The Reaction of Metal Oxides with Aquated Chromium(II) Ion," *Inorg. Chem.* **3**, 963–968.